PneuModule: Using Inflatable Pin Arrays for Reconfigurable Physical Controls on Pressure-Sensitive Touch Surfaces

Changyo Han, Ryo Takahashi, Yuchi Yahagi and Takeshi Naemura
The University of Tokyo
Tokyo, Japan
{hanc, rtakahashi, yahagi, naemura}@nae-lab.org

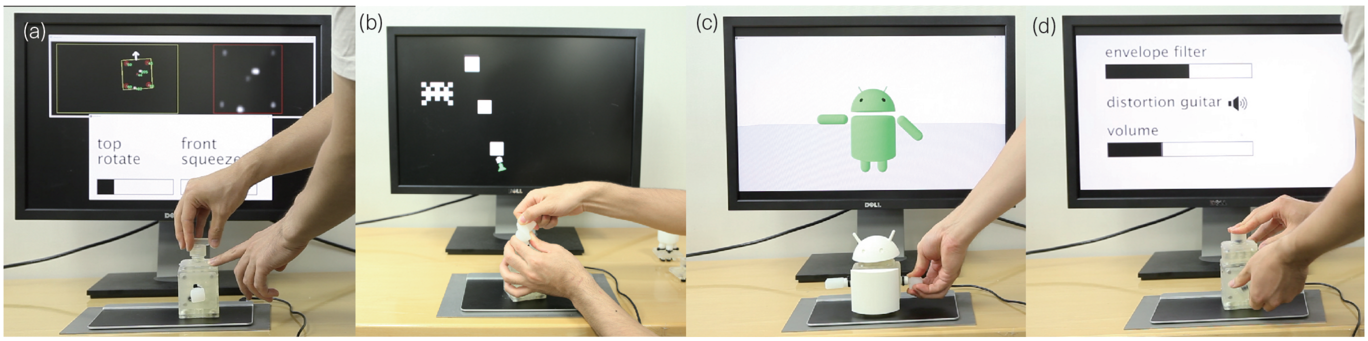

Figure 1. PneuModule and example applications. (a) PneuModule provides a tangible interface platform that allows users to quickly reconfigure the layout of physical controls that support rigid or deformable input. The modularity of the system is achieved through a combination of inflatable pin arrays and pressure-sensitive touch surfaces. We show the versatility of our system with (b) a reconfigurable game controller, (c) an interactive toy character, and (d) an adaptive music controller for sound exploration.

ABSTRACT
We present PneuModule, a tangible interface platform that enables users to reconfigure physical controls on pressure-sensitive touch surfaces using pneumatically-actuated inflatable pin arrays. PneuModule consists of a main module and extension modules. The main module is tracked on the touch surface and forwards continuous inputs from attached multiple extension modules to the touch surface. Extension modules have distinct mechanisms for user input, which pneumatically actuates the inflatable pins at the bottom of the main module through internal air pipes. The main module accepts multi-dimensional inputs since each pin is individually inflated by the corresponding air chamber. Also, since the extension modules are swappable and identifiable owing to the marker design, users can quickly customize the interface layout. We contribute to design details of inflatable pins and diverse pneumatic input control design examples for PneuModule. We also showcase the feasibility of PneuModule through a series of evaluations and interactive prototypes.

CHI '20, April 25–30, 2020, Honolulu, HI, USA

DOI: https://doi.org/10.1145/3313831.3376838

Author Keywords
Tangible user interfaces; pressure-sensitive touch surfaces; pneumatic actuation; reconfigurable physical controls

CCS Concepts
•**Human-centered computing** → **Human computer interaction (HCI);**

INTRODUCTION
The majority of human-computer interface devices have rigid shapes and do not allow room for end-user adaptation. We believe that the user experience is improved with a *flexible* user interface that adapts its shape and functionality according to the application. This vision has been proposed by Villar *et al*. [42], and several studies have investigated the feasibility of reconfigurable physical interfaces [42, 30, 17, 34, 19, 7]. The reconfigurable physical interfaces are desired to employ passive and untethered physical controls since they allow users to iterate over various interface designs easily and quickly at low cost and without worrying about the battery maintenance [15, 34]. However, there are concerns about limited input modality since most systems usually provide rigid physical controls such as buttons, knobs.

To address this limitation, recently, a large body of research in human-computer interaction field focuses on the potential of non-rigid interactions (*i.e.,* deformable user interfaces) [4]. Different from rigid user interfaces, deformable user interfaces which afford input modalities such as squeezing, bending, and twisting, allow users to experience richer interactions for gaming [40] or music performance [39, 38] and so on. Therefore, we aim to create a reconfigurable physical interface that supports both rigid and deformable input.

One promising way is to employ interactive surfaces that allow passive tangible objects to accept deformable user input [33, 16]. Because these surfaces can recognize the deformation state of the tangibles by monitoring their footprints, which are designed to respond to user input. However, since previous methods [33, 16] work on the capacitive touch surfaces, the system's behavior is 1) significantly affected by the grounding condition which may require a calibration process for individuals, or 2) vulnerable to the surrounding dielectric environment. In contrast, we focus on pressure-sensitive touch surfaces that can afford interactions through any non-conductive and soft tangible objects [32, 22]. Also, such surfaces provide the possibility to utilize material stiffness to facilitate kinetic interactions [13].

To push the boundaries of reconfigurable physical interfaces, this paper introduces PneuModule, a platform for reconfigurable physical interfaces that support both rigid and deformable user input. PneuModule operates on pressure-sensitive touch surfaces by leveraging pneumatically-operated inflatable pin arrays, as shown in Fig 1. PneuModule consists of two types of modules: a main module and extension modules. The main module can be tracked on the surface owing to its unique footprint. The extension modules allow the main module to accept physical input of various modalities. When an extension module is connected to the main module, the main module's internal air pipes link the inflatable pins at the bottom of the main module to the extension module's air chambers. With this configuration, physical input can be forwarded to the touch surface. Since the inflatable pins are isolated from each other, the main module can also accept multidimensional input. In addition, the pins can be used to represent the ID of the extension module: This allows users to reconfigure the interface layout instantly.

The main contributions of this work can be summarized as follows:

1. Design of pneumatic mechanism that effectively transmits physical input to the pressure-sensitive touch surface, and supports both rigid and deformable input.
2. Marker and connector designs that realize the modularity of the system.
3. A variety of example applications implemented by the proposed system.

In the following sections, we will describe related work, design and implementation details of PneuModule, potential applications, technical evaluations, limitations, and future work.

RELATED WORK

Our work is mainly related to the following research fields: 1) reconfigurable physical interfaces, 2) tangibles on interactive surfaces, and 3) deformable interfaces.

Reconfigurable Physical Interfaces

Unlike graphical user interfaces (GUI), physical controls like buttons, knobs, and sliders provide richer tangible experience through their shapes, motions, and materials [28]. However, the physicality of such controls makes them difficult to be customized since physical interfaces often come with a rigid shape and a fixed layout. To resolve this limitation, several development tools have been proposed that allow users to customize physical controls with less time and effort [42, 8, 21, 34].

To enhance customizability, such system requires both 1) quick reconfiguration of interface layout and 2) sensing the state of physical controls without tethered wires. For example, MagGetz [15] showed that using the embedded magnetometer to wirelessly analyze magnet-augmented physical controls around a smartphone. Also, RFIBricks [14] used magnet-triggered RFID switches and an RFID reader array to create interactive building blocks that are aware of their 3D position, orientation, and applied user input. While these studies allow users to rapidly configure physical controls, the input modality is limited by the use of off-the-shelf physical controls and thus, cannot support deformable input. In contrast, PneuModule supports deformable input modalities by using a pneumatic mechanism, as well as enabling the reconfiguration of the modules with a dedicated marker and connector design.

Tangibles on Interactive Surfaces

One of the promising ways to achieve tangible user interfaces is to employ interactive surfaces that can identify, localize, and sense tangible objects [45, 6, 48, 44, 9, 43, 3, 11, 24, 23]. Among many interactive surface technologies, capacitive touch surfaces are most accessible since they are equipped with most modern devices. Recently, some studies have attempted to attribute deformable input capabilities to passive tangibles on capacitive touch surfaces. For example, Flexibles [33] are 3D-printed passive tangibles that support various deformable inputs by using the geometric change of electrodes inside the tangibles. Also, Ohmic-Touch [16] uses resistance change of the on-surface tangibles embedded with force-sensing resistors to support deformable input. However, as noted above, these approaches share common limitation of using capacitive touch sensors that make the system vulnerable to the surrounding dielectric environment and grounding conditions.

On the other hand, pressure-sensitive touch surfaces have advantages that they can capture the contact of any tangible objects [13, 5, 32, 11, 22, 10]. For example, GravitySpace [5] and Kickables [32] used frustrated total internal reflection (FTIR)-based pressure sensing floors to sense human postures and footprint of marker-embedded furniture. Also, Geckos presented magnet-augmented fiducials that enable various pressure interactions on vertical walls [22]. However, as Branzel *et al.* pointed out, pressure sensing through tangible objects limits the user input capabilities to a manipulation of overall weight and balance of the objects [5]. PneuModule, on the other hand, attempts to overcome this limitation by employing pneumatically-actuated pin arrays on passive tangible objects; this can easily forward the physical inputs through air pipes, which will be described in the following section.

Deformable Interfaces

Deformable interfaces are one of intuitive interactions in everyday life and enable users to extend input modalities beyond conventional rigid interfaces (*e.g.*, deformable game controller) [4]. A body of research has utilized optical [12, 29], resistive [35, 25, 26, 47, 16, 18], capacitive [33, 46, 27], acoustic [20], or pneumatic system [35, 41] to capture the deformation of objects. Among them, pneumatic physical controls have advantages that their behavior can be captured at a distance via air pipes, and also they can afford various physical manipulations [41]. Taking advantages of the pneumatic systems, PneUI explored soft composite materials that can be used for shape-changing interfaces [46]. Slyper *et al.* presented a set of pneumatic design to enable various deformable user inputs like squeezing, twisting, bending and so on [35]. While the work of Vázquez et al. [41] allows users to 3D print customized pneumatic controls, the system requires complex air tube connections and barometric pressure sensors for input detection; thus, hinders the reconfigurability of the controls. Building on these researches, PneuModule aims to build a modular platform that enables instant reconfiguration of deformable input controls; we create tangible objects with built-in pneumatic mechanisms that forward user input to pressure-sensitive touch surfaces.

GENERAL CONCEPT OF PNEUMODULE

Based on the above discussion, there are three requirements for designing PneuModule:

1. Pneumatic mechanism to effectively transmit user input to the pressure-sensitive surface.
2. Modular design for instant interface layout reconfiguration.
3. Module tracking on the touch surface.

To address the first requirement, we investigated design parameters of inflatable pins to obtain a sufficient amount of inflation. In addition, we analyzed and determined the parameters that affect pin inflation were For the second and third requirements, we introduced a marker design that allows simultaneous sensing of the connected extension modules and their physical inputs while tracking the main module.

The remainder of this section describes an overview of the system design that resolves the aforementioned issues. All of the resulting implementation details (3D CAD models, materials, software, applications) are made available under the MIT license[1].

Design Overview

Fig. 2 (a) shows an overview of the PneuModule system. The system consists of three main components: 1) a main module, 2) extension modules, and 3) a pressure-sensitive touch surface. At the bottom of the main module, there are dozens of inflatable pins which can be actuated by air pressure applied to the connected air pipes. When an extension module is connected to the main module, the corresponding pin can be actuated pneumatically by the pressure increase in the extension module's air chamber. Therefore, the inflated pins make contact with the pressure-sensitive touch surface, allowing the system to capture a continuous pressure input. Also, some pins in predetermined locations can be used to identify the type of the connected extension module: This allows users to quickly customize the functionality of PneuModule. Besides, we arrange a metal plate at the rear of the pressure-sensitive touch surface to allow the module to stick to the surface, similar to Geckos [22].

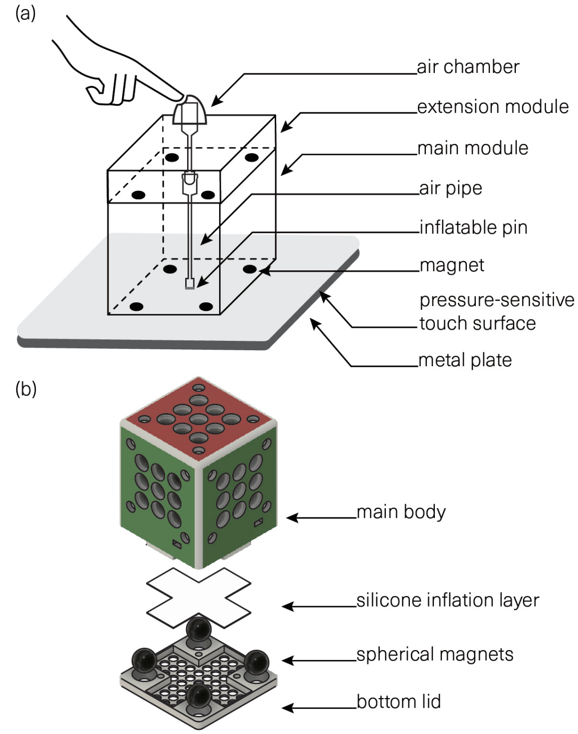

Figure 2. A system overview of PneuModule. (a) Our system consists of 1) a main module, 2) extension modules, and 3) a pressure-sensitive touch surface. Users can customize the function of a main module by connecting diverse extension modules to the main module. When connected, the pressure change in the extension modules' air chambers alters the footprint of the main module, thus enabling the touch surface to recognize user input through the extension modules. (b) Exploded view of the main module.

Main module can be made of four independent parts: a main body, a silicone inflation layer, four spherical neodymium magnets, and a bottom lid as shown in Fig. 2 (b). As a prototype, the main module has a cubic shape, and extension modules can be connected to one of five sides of the main module. The silicone inflation layer and the magnets are sandwiched between the bottom of the main body and the bottom lid. The inflation layer is divided into circular inflatable pins by the holes on the main body and the bottom lid. There are number of internal air pipes that connect extension modules' air chamber to the inflatable pins. The magnets are used as reference points for tracking the main module. In addition, the magnets keep the gap between the inflation layer and the surface, which prevents the main module from floating off the touch surface due to repulsion from the inflated pins.

[1] https://github.com/hanchangyo/pneumodule

MAIN MODULE DESIGN AND IMPLEMENTATION

We show the design of the main module from three aspects: 1) marker design, 2) inflatable pin design, and 3) socket and internal air pipe design. Then, we explain the implementation process of the main module.

Marker Design

First, we describe the marker design of the main module. The marker structure allows the pressure-sensitive touch surface to 1) capture the physical input and the ID of the extension modules and 2) track the main module on the surface. To analyze the connected extension modules, we arranged 45 pins at the bottom, as shown in Fig. 3 (a). The pins in the red-colored area accept inputs from the top side, and green-colored areas correspond to the inputs from front, back, left and right sides. For each pin, we can assign whether the pin is used for sensing or for identification. As an example, we assigned the pins at the corner of 3×3 grid as identification pins (ID pins), as shown in Fig. 3 (b). The rest of the pins are assigned for sensing the pressure input from the extension modules. Based on this pin assignment, we can detect the type of extension modules up to 15 ($=2^4 - 1$) and also sense up to five individual pressure inputs for each extension module. The pin assignment can be rearranged depending on the application purpose: for example, if we need to identify more number of extension modules, we can assign more pins for ID.

Next, we explain the tracking approach of the marker attached to the main module. To allow the system to track the main module, we arranged the four magnets at the vertices of a right trapezoid, as shown in Fig. 3 (a); the point asymmetry of the magnets allows the surface to track the position along with the orientation of the main module. Fig. 4 explains the tracking and input recognition process when the four extension modules are connected to the main module (See Fig. 4 (a)). At first, the system monitors the captured pressure image and finds representative points (blobs) which are composed of four magnets (See Fig. 4 (b)). The edge lengths and the angles are predetermined for the magnet points, so we can find the marker position from the obtained blobs (See Fig. 4 (c)). After the marker area is determined, we split the marker region into five areas to separate the inputs coming from different sides (See Fig. 4 (d)). By monitoring the intensity of the pressure image, continuous pressure values for each pneumatic actuation can be obtained from the extension modules as shown in Fig. 4 (e). We can also identify the connection state of the extension modules by checking the actuated ID pins.

Inflatable Pin Design

Important design parameters that determine the dimension of the main module are illustrated in Fig. 5. Determine the parameters requires investigation of the inflatable pins' inflation characteristics, as they play a role in forwarding physical input to the surface. The inflation characteristics of a flat, inflatable pin are mainly affected by three factors: 1) stiffness, 2) thickness, and 3) diameter. First, to examine how the stiffness affects the inflation, we fabricated a 1 mm-thick silicone layer with the Ecoflex™ 00-30[2] (Shore hardness 00-30), and set the pin diameter to 3.5 mm. However, since the material was too elastic, the pin inflated 5.6 mm to the axial direction and 7.6 mm to the radial direction even with 1.6 atm of pressure. This caused the interference between adjacent pins as shown in Fig. 7 (a); due to this, it is concerned that the pressure-sensitive touch surface cannot distinguish the adjacent pins.

[2]Smith-On Inc., https://www.smooth-on.com/products/ecoflex-00-30/

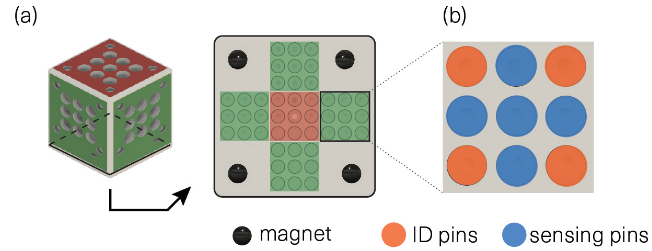

Figure 3. An overview of the marker design of the main module. (a) Isometric view and bottom view of the main module. To enable both sensing and identification of the extension modules, we arranged a 3×3 inflatable pin array for each side, and (b) the example configuration shows that each array has five pins for sensing (blue-colored circle) and four pins for identification (orange-colored circle).

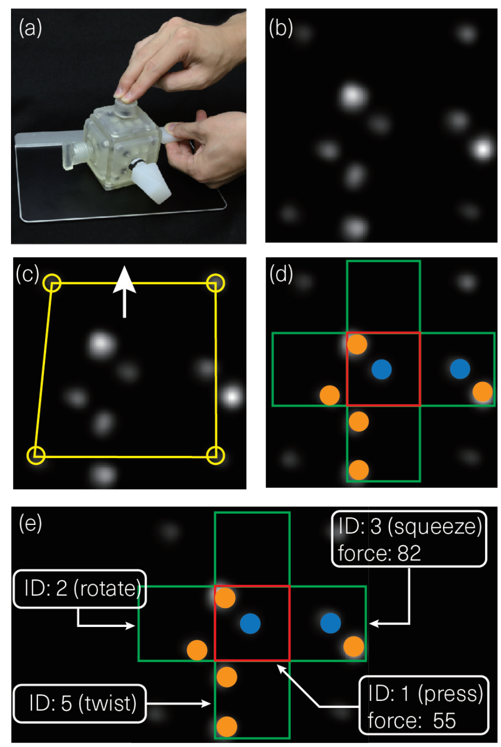

Figure 4. An overview of the tracking approach of the main module. To illustrate our tracking approach, we prepared (a) a main module which has four connected extension modules and (b) the captured pressure image by the pressure-sensitive touch surface. (c) First, the pressure-sensitive touch surface detects the magnet footprint (illustrated as yellow circles). The asymmetric footprint (yellow edges) allows the system to recognize the orientation of the main module. (d) Then, the detected marker region is split into five areas, and we detect the position of the sensing pins (blue circles) and the ID pins (orange circles). (e) Finally, the system identifies the extension modules and captures the user inputs by monitoring the pressure value of the blobs at the location of the sensing pins.

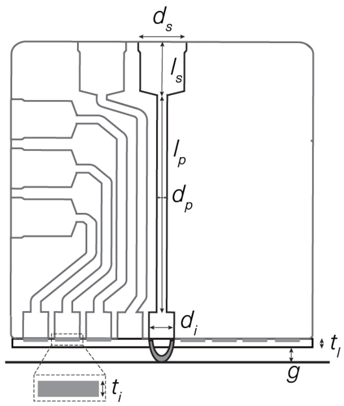

Figure 5. Design parameters of the main module. d_s: socket diameter, l_s: socket length, d_p: pipe diameter, l_p: pipe length, d_i: inflatable layer diameter, t_i: inflatable layer thickness, t_l: bottom lid thickness and g: gap between the bottom lid the touch surface.

Table 1. Design parameters of the main module.

Parameters	d_s	l_s	l_p	d_i	t_i	t_l	g
Value (mm)	8.8	10	30-65	5	1	0.4	0.5

Also, over-inflation against axial direction causes shear deformation when the main module slides on the surface (See Fig. 7 (b)), which causes positional misalignment from the magnet positions and thus, the surface cannot recognize the position of the pins correctly. To cope with the two problems above, we use relatively stiffer two-part silicone (HTV-2000[3], Shore hardness 18A).

Next, we conducted experiments to investigate how the thickness and the diameter affect the inflation as shown in Fig. 6. We prepared 3D-printed test rigs of three different hole diameters (3 mm, 4 mm, 5 mm) and two different thickness of cast silicone layer (0.4 mm and 0.6 mm). We measured the height of the pin by monitoring the volume markings (See Fig. 6 (a)) and captured sensor output (See Fig. 6 (c)) while applying the pressure with a syringe. The test rigs in Fig. 6 (c) had three small feet (height: 0.5 mm) and the thickness of the bottom lid was 1 mm. Although it is desirable to reduce the gap between the inflatable pins and the touch surface to lower the activation force, the gap was limited to 1.5 mm since the printed bottom lid with 0.5 mm thickness was too brittle so broken easily.

As a pressure-sensitive touch surface, we have chosen to use Sensel Morph[4], an off-the-shelf pressure-sensitive touch surface that provides access to raw pressure image via provided API. It has a 2D array of 19,425 (185 columns×105 rows, 1.25 mm pixel spacing, 240 mm×169.5 mm) pressure sensors. Each touch point has a dynamic range of 30,000 levels and can measure forces from 0.005 kgf to 5 kgf.

Fig. 6 (b) shows the height of the pin in various thickness-diameter conditions. Owing to the stiffness of the material, the pins did not inflate much to the radial direction so we measured the height only. The pressure values were calculated from the syringe volume using Boyle's law ($PV = k$). We confirmed that an inflatable pin of 5 mm diameter and 0.4 mm thickness could touch the surface at the lowest pressure than any other conditions. Also, this design showed the most sensitivity when captured by the touch surface as shown in Fig. 6 (d). Therefore, we determined to utilize the parameters (See Table. 1, g: 0.5 mm, t_l: 1 mm, t_i: 0.4 mm, d_i: 5 mm) for the inflatable pins in our prototype.

[3]Engraving Japan, http://www.engravingjapan.com/
[4]Sensel Morph, https://sensel.com/

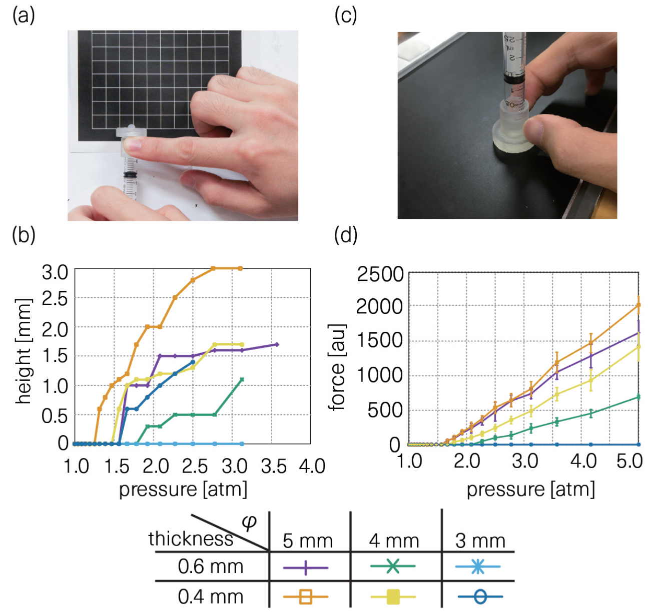

Figure 6. (a) An experiment setup to measure the height of the inflatable pins. (b) The height of the inflatable pin with applied air pressure. We changed the pressure between 1 atm and 5 atm using a syringe. (c) The experiment setup to measure the force applied to the pressure-sensitive touch surface via inflated pins, and (d) the results of the relationship between the compressed pressure and the applied force.

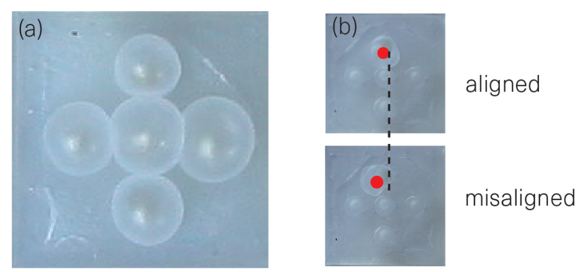

Figure 7. Problems of over-inflated pins. (a) The footprints of the pins are not isolated from adjacent pins since they interfere with each other. (b) If the main module slides on the surface while the pins are inflated, positional misalignment occurs.

Socket and Internal Air Pipe Design

Next, we explain the design of the internal air pipes which connect the inflatable pins to the air chambers of extension modules. Inside the main module, as illustrated in Fig. 8 (a), a thin internal air pipe connects a socket to an inflatable pin. The main module has multiple sockets (3×3) on each side except the bottom. There are two types of plugs that insert into the main module as shown in Fig. 8 (b). Thru-hole plugs, which

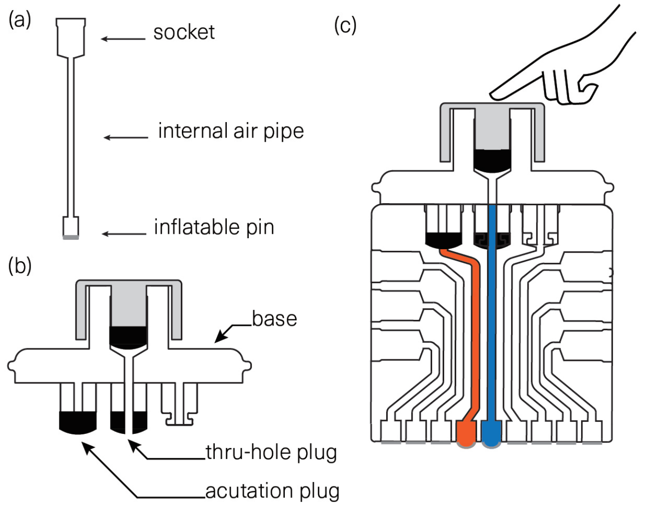

Figure 8. (a) The design of the internal air pipe in the main module. The pressure change caused by compressed internal volume pneumatically actuates inflatable pins via thin pipes. (b) There are two types of plugs for connection: thru-hole plugs and actuation plugs. (c) A thru-hole plug passes the airflow from the extension modules' air chamber (blue). In contrast, an actuation plug inflates ID pins when connected (orange).

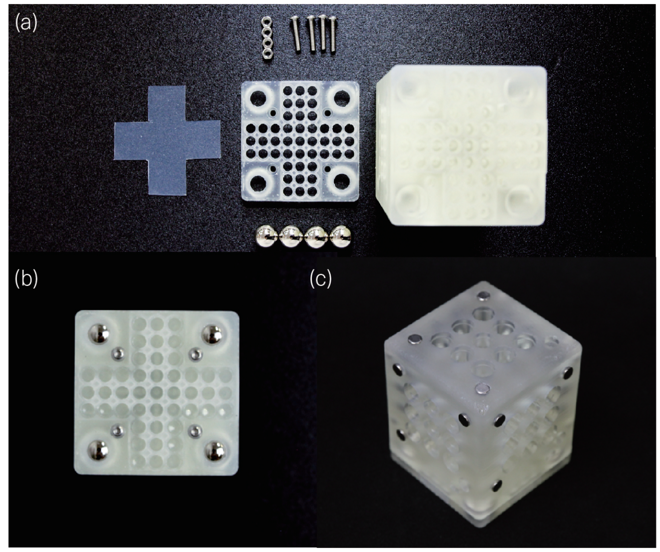

Figure 9. The illustration of the implemented main module. (a) The parts of the main module: a bottom lid, a silicone inflation layer, four magnets, bolts and nuts, and a main body. (b) The bottom view and (c) the isometric view of the main module. We implemented 45 (=$3 \times 3 \times 5$) inflatable pin arrays at the bottom of the main module and 9 (=3×3) connectors on each of the other sides.

have small holes in the center, allow the air from the extension module's air chamber to pass through. In contrast, actuation plugs (no holes) are used to actuate the identification pins of the main module. Inserting the actuation plug compresses the air in the socket and actuates the corresponding inflatable pin. We determined to use syringe plunger tips (TERUMO SS-02SZ, tip diameter: 8.8 mm) as plugs since they are inexpensive and readily available for airtight connection. Thus, the socket diameter d_s is determined to 8.8 mm to fit the plug. There are individual connections realized by internal air pipes between the sockets and the pins as shown in Fig. 8 (c). When no extension modules are connected, the inflatable pins stay flat. When the extension module is connected, the actuation plugs inflate the pins representing the ID of the module (annotated as orange in Fig. 8 (c)). Furthermore, when the user input is applied, the pressure in the air chamber of the extension module activates the corresponding inflatable pin via the thru-hole plug.

Since the inflation of a pin is determined by the difference between the initial volume and the compressed volume, we can calculate the internal pressure from the volume change. When an actuation plug is fully inserted into the socket, the internal pressure P' can be calculated as

$$P' = P\frac{V_s + V_p}{V_p}, \tag{1}$$

where P is the initial pressure (atmospheric pressure), V_s is the volume of the socket, and V_p is the volume of the pipe. Since the pressure can be increased by reducing the volume of the internal air pipes, we set the diameter of the air pipe as 2 mm, which is slightly larger than the minimum hole diameter that the 3D printer can print. The socket length l_s was determined to be 10 mm, to avoid the interference from the sockets on other sides. The lengths of the routing pipes varied from about 30 mm to 65 mm depending on the position of the corresponding socket: This results in the internal pressure of 3.89 atm to 5.34 atm, which is enough for the pin to reach the touch surface with enough force according to the results in Fig. 6. Based on these experiments and observations, we determined the design parameters for the main module (See Table 1).

Implementation of Main Module

Fig. 9 shows the implemented prototype of the main module. We constructed the main module using five parts: a main body, a bottom lid, a silicone inflation layer, four spherical magnets, and bolts and nuts as shown in Fig. 9 (a). First, to fabricate rigid parts (the main body and the bottom lid), we used a stereolithography 3D printer (Formlabs Form 2[5]) with UV curable clear resin, to ensure the parts to be airtight. We avoided using FDM printers since they are not suitable for making airtight parts due to gaps between layers. Then, we attached the silicone layer to the bottom of the main body with a special adhesive (Cemedine PPX), since the silicone is difficult to adhere to other materials. Also, we put the spherical magnets to the holes and secured the bottom lid with bolts and nuts (See Fig. 9 (b)), and also attached cylindrical neodymium magnets asymmetrically to constrain the orientation of the extension modules (See Fig. 9 (c)). Based on the above fabrication process, the size and weight of the main module were 60 mm×60 mm×72 mm and 290 g, as shown in Fig. 9 (c).

EXTENSION MODULE DESIGN AND IMPLEMENTATION

To demonstrate the versatility of our design, we implemented functional prototypes of the extension modules, as shown in Fig. 10. We categorized and fabricated extension modules based on the modality of the physical input. Note that the operating pressure range of a pneumatic control can be adjusted by

[5] Formlabs Form 2, https://formlabs.com/

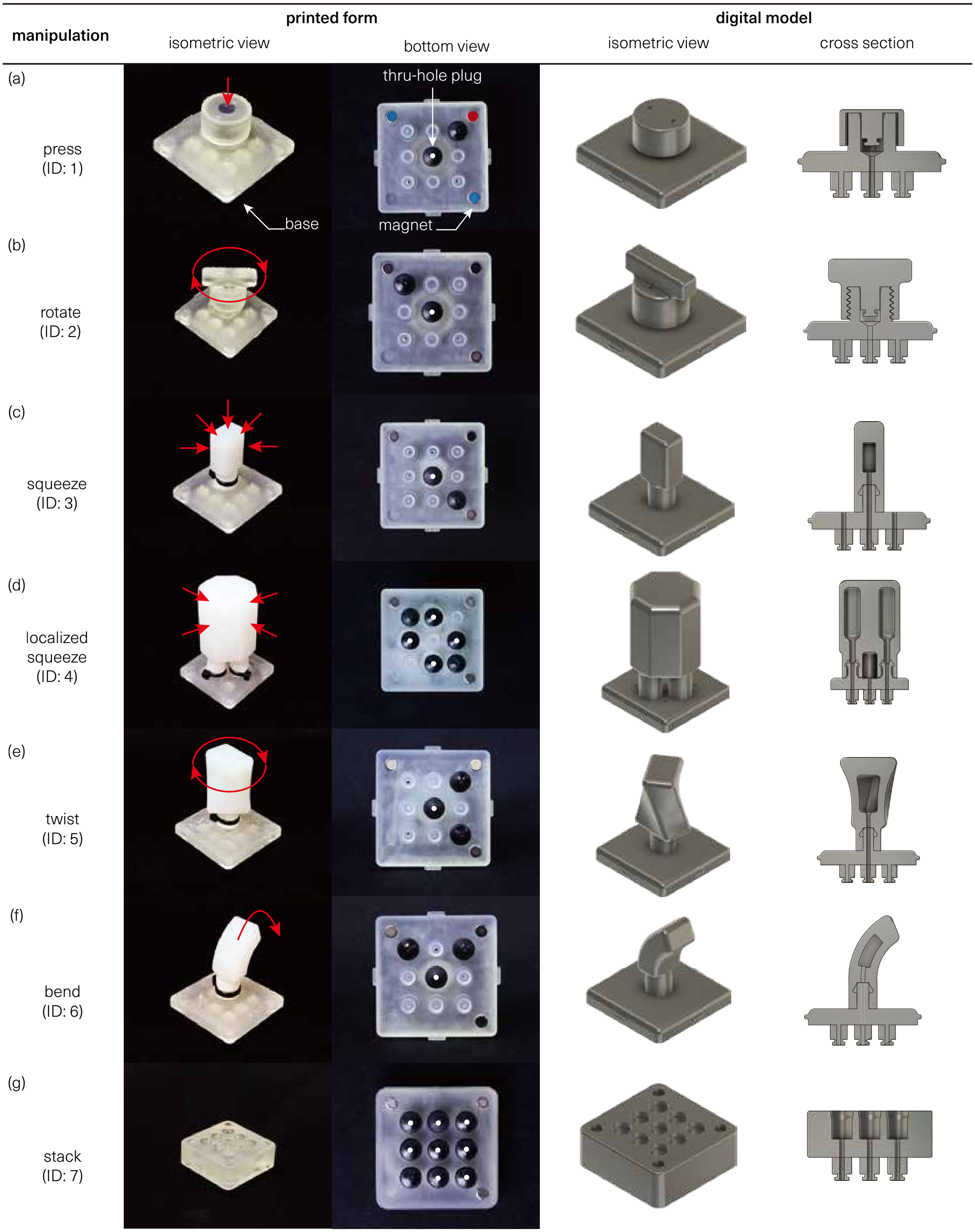

Figure 10. Our set of extension modules for prototyping physical inputs. We implement seven extension modules, each of which enables users to (a) press, (b) rotate, (c) squeeze, (d) localized squeeze, (e) twist, (f) bend, and (g) stack the modules. Each module has both the unique ID and internal air pipe.

changing the volume of the air chamber. This is an advantage of pneumatic device controls for prototyping in comparison to mechanical counterparts [41]. Also, we assigned four pins at the corners of 3×3 grid to represent module IDs, shown in the bottom view of Fig. 10. To prevent the extension module from popping out from the main module, we used cylindrical magnet connectors (NSN in clockwise) to constrain the orientation of connection. Still, a wrong orientation of 180 degrees cannot be prevented, a possible improvement is to place the sockets asymmetrically.

The fabrication process of extension modules are described below. The rigid input modules (*i.e.*, press and rotate module) consist of a base and rigid input parts, whereas the deformable input modules are composed of a base and a deformable input part. The base and rigid input part of the module are 3D printed (Formlabs Form 2, clear resin), and the deformable input part is made of cast silicone (HTV-2000). In order to create the internal air chamber (*i.e.*, deformable input part) by silicone casting, first, we printed a water-soluble mold by an FDM printer. Then, we poured the two-part silicone mixture into the mold, and finally, we dissolved the mold in the water after curing. After this fabrication process, the deformable input part was inserted into the barbed fitting on the base, then zip-tied to keep the chamber airtight. The volume and geometry of the air chamber can be designed to change the sensitivity according to Eqn. 1.

Press
A press module has a linear sliding motion, and can be pressed like a normal button as shown in Fig. 10 (a). This module consists of a rigid base with an air chamber and a rigid button cap. When users press the button, the actuation plug equipped on the button cap compresses the air, and thus inflates the sensing pin at the bottom of the main module. The button returns to its initial position since the compressed air pushes the button cap back when users release the button.

Rotate
A rotate module has an air chamber similar to the press module, but has a threaded handle that fits the base of the module (Fig. 10 (b)). When the handle rotates clockwise, the actuation plug goes toward the bottom of the air chamber, pushing out the air to the corresponding inflatable pin. This mechanism converts the user's rotation motion to the linear motion while giving a continuous state of the rotation.

Squeeze
For a basic deformable input, we created a module that accepts squeeze input (Fig. 10 (c)). This module was designed to effectively respond to pinch input from a specific direction by making the chamber size asymmetric in width and depth.

Localized Squeeze
By using multiple sensing pins, we can also create extension modules that can accept multidimensional, localized inputs. As an example, we fabricated a module that accepts squeeze input from multiple directions, as shown in Fig. 10 (d). It has four separate air chambers on each side of the handle, so this module can identify the squeezed direction (See Fig 11).

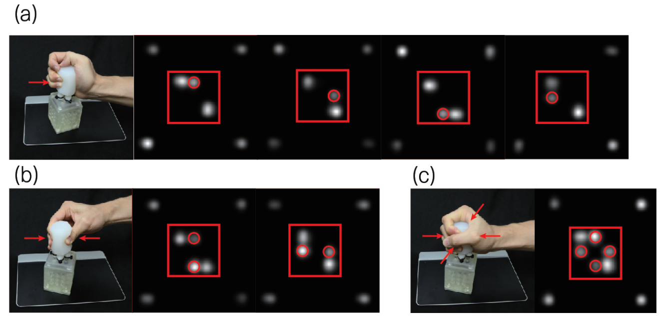

Figure 11. Operation of the localized squeeze module. (a) It accepts a single squeeze comes from four different directions, (b) also aware of two inputs from opposite directions, (c) and four directions.

Twist
A twist module is designed to be easily twisted in only one direction as shown in Fig. 10 (e). It has an air chamber where a large air compression occurs when twisted.

Bend
We also fabricated an extension module that can accept a bend input as shown in Fig. 10 (f). Although it has similar geometry to the squeeze module, but it has an air chamber where crease happens when bent. Obviously this module also responds to both squeeze and bend input, its shape will encourage the bend motion [35]; we will deal with it by developing the specific mechanism which only responds to the bend motion in the future work.

Stack
A stack module can be inserted between an input extension module and the main module (See Fig. 10 (g)). It has no input function, but has an actuation plug for the redundant ID pin (lower left) to alter the ID of the connected extension module. For other pin positions, there are thru-hole plugs which can pass the airflow from the connected extension modules. Therefore, the stack module allows users to alter the ID of an extension module without changing the input function of the extension module. In addition, we can resolve the physical order of multiple stacked modules by encoding the pipe routing, bringing another possible interaction [2, 6, 3]. However, there is a trade-off between the number of stack modules and the pressure operating range. Multiple stacks increase the initial volume with additional air pipes. This changes the pressure operating range and limits the maximum number of stacks.

APPLICATION EXAMPLES
Reconfigurable Game Controller
The first example is a shooting game with a tangible controller, inspired by Space Invaders[6] . Users can move the spaceship by sliding the main module horizontally across the touchpad and fire at the invading aliens by applying input to connected extension modules. The spaceship can equip three distinct weapons on its front, left and right, which can be done by connecting different extension modules at the corresponding side of the

[6]Our implementation is based on "Space Invaders in Processing 3" by Gabriel: https://gist.github.com/ihavenonickname/5cc5b9b1d9b912f704061a241bc096ad

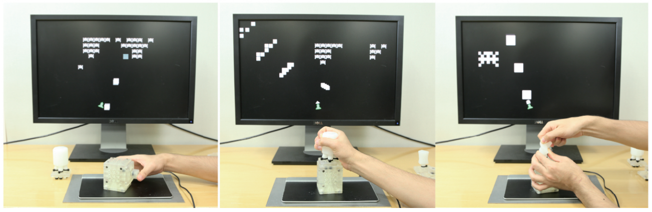

Figure 12. A reconfigurable game controller. Users can physically swap the attached weapons: left: a normal shot, middle: a directional multi-shot, and right: a charge shot.

Figure 13. An interactive toy character. Users can interact with virtual Bugdroid through the tangible avatar by left: pressing the head and middle: pinching the arms. right: Also, the motion of the character can be changed by replacing the arm part (squeeze) with another one (bend).

Figure 14. An adaptive music controller. left: Users can press the button to play a clean guitar sound, and middle: the sound can be changed by inserting a stack module (distortion effect). Right: we can add another function (volume knob) easily on the other side.

main module. We implemented three different shots which utilize characteristic of the extension module's input modality, as shown in Fig. 12. Users can pick the most adequate weapon depending on the gameplay situation. While the reconfigurable game controllers presented in previous work [42] provides a way to implement deformable inputs (*e.g.*, using pressure transducers), PneuModule enables users to add deformable input controls in a much easier way by simply swapping the extension modules. Future implementations may include co-operative gameplay using a limited number of input modules to encourage interaction between players.

Interactive Toy Character

Previous studies have shown that toys can be made interactive when incorporated with deformable input capabilities [25, 37, 26, 33], but by making them instantly reconfigurable, users can explore the interaction design in real-time. To support such demands, we created an interactive toy character using PneuModule. This toy not only accepts user input, but also provides different tangible interactions by customization. Fig. 13 shows an example of the interactive toy character, Bugdroid[7]. Users can interact with virtual character on the screen through the tangible avatar. They can press the head to shrink the neck, and alter the motion of the arm by swapping it with another one (*e.g.*, stretching motion to bending motion).

[7] "The Android robot is reproduced or modified from work created and shared by Google and used according to terms described in the Creative Commons 3.0 Attribution License."

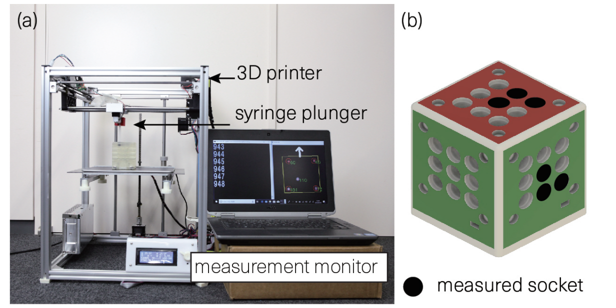

Figure 15. The experiment setup for our durability test. We used a 3D printer to inflate and deflate the inflatable pin repeatedly and observed the moment when the pin breaks using the obtained pressure image.

Adaptive Music Controller

For musicians who explore sound or do musical improvisations, tabletop tangible interfaces are considered to support the activity of *sketching musical ideas* [1]. Building upon this idea, we created an adaptive music controller that allows tangible sound manipulation as shown in Fig. 14. Diverse sound samples or effects can be mapped to different physical controls, enabling dynamic sound exploration. For example, we mapped the press button module to playback a clean guitar sound. The horizontal position of the module changes the center frequency of the envelope filter. The stack module turns the clean guitar tone into a distorted sound, providing a tangible representation of the sound effect. In addition, users can attach the rotate module for adjusting the sound volume.

EVALUATION

Here, we conducted a series of evaluations to confirm the performance of PneuModule. First, we evaluated its durability. Then, we investigated the accuracy of the set of physical input mechanisms (press, rotate, and twist input).

Durability of Inflatable Pins

First, we tested the durability of the inflatable pin of the main module. In this test, we counted the number of times the inflatable pin can be inflated and deflated without break. As shown in Fig. 15, we used a 3D printer to inflate and deflate the inflatable pin repeatedly and observed the moment of the pin break by monitoring the pressure image obtained by the touch surface. Here, we examined the durability of the pins at 6 socket positions considering the point symmetry of the main module. In one measurement cycle, the pin was inflated for 1 s and then, the pin was deflated for 1 s. Under this condition, we applied about 3.89 atm to 5.34 atm depending on the pin position, which is necessary at minimum to contact the inflated pin on the surface, as shown in Fig. 6(b). The result indicates that the pins inflated 2392 (mean)$\pm$1062 (SD) times without breaking, which is feasible during prototyping with PneModule. However, to reach the durability level of a commercially-available mechanical switches, it may need to endure more than a few million times of inflation. Also, the relatively large variation of break times might be due to non-uniformity caused by the manual adhesion process of the silicone inflation layer.

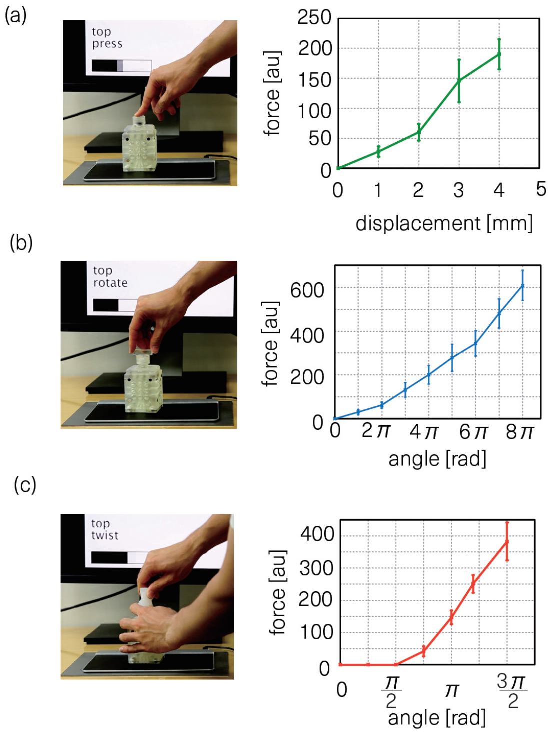

Figure 16. We measured the accuracy of the available physical inputs for PneuModule. We plotted the mean and the standard deviation of the measured force for (a) press input, (b) rotate input, and (c) twist input.

Accuracy of Physical Inputs

Next, we evaluated the accuracy of press, rotate, and twist inputs; note that we have only evaluated these modules since they can be measured under relatively controlled conditions than other modules (squeeze and bend). For a press module, we measured the relationship between the displacement and the force applied to the pressure-sensitive touch surface, whereas, for rotate and twist modules, we measured the relationship between the rotation angle and the force. We measured the force at randomly selected 10 positions on the pressure-sensitive touch surfaces and calculated the mean and the standard deviation of the applied force for each input. The measurement step of the displacement of press motion was 1 mm, whereas, the step of the rotation angle of rotate or twist input was π or $\pi/4$, respectively. Fig. 16 (a), (b), and (c) respectively show the measurement result of press, rotate, and twist module. The results indicate that the measured force values varied according to the manipulated displacement of the physical controls. However, due to the relatively large standard deviation, a slight level of pressure change cannot be distinguished. The cause of the standard deviation is due to the interpolating behavior of the Sensel Morph; even though this makes it possible to estimate the force value between force sensor arrays in the pressure-sensitive touch surface, the values at such areas are not reliable [36].

LIMITATIONS AND FUTURE WORK

Module Geometry

In this paper, we designed the geometry of the main module as a cuboid, since it is one of the primitive geometries that can be easily reconfigured like LEGO®. We do not claim to constrain the shape of the module, as for other applications, other shapes may be more appropriate for interaction. With concerning that complex shapes might increase the complexity of routing internal air pipes, we plan to create algorithms that automatically route them as presented in [31].

Module Scalability

In our prototype, the size of the main module is restricted by two factors: 1) the resolution of the pressure-sensitive touch surface and 2) the inflation characteristics of the inflatable pins. The major factor was the latter one since the pins should be inflated more than 1.5 mm (the gap between the pins and the surface) to activate the surface. This requires sufficient socket volumes which can be inferred from the Eqn. 1 and the measured inflation characteristics. For placing 3×3 sockets on each side, the side length of the main module had to be about 60 mm, which might not be suitable for some applications (*e.g.*, tangible CAD application). By reducing the gap, we expect the size of the module decreases as well as lowering the required pressure force for activation.

Surface Friction

The modules only work when they are on the touch surface, so they cannot be lifted so the surface friction can be a problem. Although we used spherical magnets to reduce the surface friction, the inflated pins increased the surface friction since they are made of cast silicone. The friction can be mitigated by applying dry lubricants (*e.g.*, talcum powder). On other aspects, we expect that the friction can also be used for emulating the weight gain of tangible objects.

Fabrication Process

In the current fabrication process, there are several processes (*e.g.*, silicone casting and assembly) that need to be performed manually by human hands. For a simplified fabrication process, it is desirable to print the assembled parts in a single pass. We attempted to print small inflatable pins merged with rigid cylinders with a multimaterial 3D printer (Stratasys Objet260 Connex), but the printed pins did not bear as much as cast silicone. As future work, we anticipate that high-resolution 3D printing technologies that can print precise multimaterial parts [49] could help the manufacturing process.

CONCLUSION

We have presented PneuModule, a reconfigurable tangible interface platform that accepts both rigid and deformable inputs using pneumatically-actuated inflatable pin arrays. We contributed to the design principle and the fabrication process of passive tangible modules with built-in pneumatic mechanisms, that operate on pressure-sensitive touch surfaces. In addition, we demonstrated the feasibility and the versatility of our system through a wide range of example physical controls with different input modalities, and a series of example applications. Our future work will include fabrication methods that leverage computational design and advanced manufacturing technologies.

ACKNOWLEDGMENTS

This work was supported by JSPS KAKENHI Grant Number JP19J14350. We also thank Yasuaki Kakehi for his considerable advice and feedback.

REFERENCES

[1] Anna Xambó Sedó. 2014. *Tabletop Tangible Interfaces for Music Performance: Design and Evaluation*. Ph.D. Dissertation. The Open University. http://annaxambo.me/pub/Xambo_2015_thesis.screen.pdf

[2] Tom Bartindale and Chris Harrison. 2009. Stacks on the surface: resolving physical order using fiducial markers with structured transparency. In *Proceedings of the ACM International Conference on Interactive Tabletops and Surfaces - ITS '09*. ACM Press, New York, New York, USA, 57. DOI: http://dx.doi.org/10.1145/1731903.1731916

[3] Patrick Baudisch, Torsten Becker, and Frederik Rudeck. 2010. Lumino: Tangible Blocks for Tabletop Computers Based on Glass Fiber Bundles. In *Proceedings of the 28th international conference on Human factors in computing systems - CHI '10*. ACM Press, New York, New York, USA, 1165–1174. DOI: http://dx.doi.org/10.1145/1753326.1753500

[4] Alberto Boem and Giovanni Maria Troiano. 2019. Non-Rigid HCI: A Review of Deformable Interfaces and Input. In *Proceedings of the 2019 on Designing Interactive Systems Conference - DIS '19*. ACM Press, New York, New York, USA, 885–906. DOI: http://dx.doi.org/10.1145/3322276.3322347

[5] Alan Bränzel, Christian Holz, Daniel Hoffmann, Dominik Schmidt, Marius Knaust, Patrick Lühne, René Meusel, Stephan Richter, and Patrick Baudisch. 2013. GravitySpace: Tracking Users and Their Poses in a Smart Room Using a Pressure-Sensing Floor. In *Proceedings of the SIGCHI Conference on Human Factors in Computing Systems - CHI '13*. ACM Press, New York, New York, USA, 725–734. DOI: http://dx.doi.org/10.1145/2470654.2470757

[6] Liwei Chan, Stefanie Müller, Anne Roudaut, and Patrick Baudisch. 2012. CapStones and ZebraWidgets: Sensing Stacks of Building Blocks, Dials and Sliders on Capacitive Touch Screens. In *Proceedings of the 2012 ACM annual conference on Human Factors in Computing Systems - CHI '12*. ACM Press, New York, New York, USA, 2189. DOI: http://dx.doi.org/10.1145/2207676.2208371

[7] Alix Goguey, Timothy Neate, Jennifer Pearson, Simon Robinson, Matt Jones, Cameron Steer, Andrés Lucero, Laurence Nigay, Deepak Ranjan Sahoo, Céline Coutrix, Anne Roudaut, Sriram Subramanian, and Yutaka Tokuda. 2019. PickCells: A Physically Reconfigurable Cell-composed Touchscreen. In *Proceedings of the 2019 CHI Conference on Human Factors in Computing Systems - CHI '19*. ACM Press, New York, New York, USA, 1–14. DOI: http://dx.doi.org/10.1145/3290605.3300503

[8] Saul Greenberg and Chester Fitchett. 2001. Phidgets: Easy Development of Physical Interfaces through Physical Widgets. In *Proceedings of the 14th annual ACM symposium on User interface software and technology - UIST '01*. ACM Press, New York, New York, USA, 209. DOI: http://dx.doi.org/10.1145/502348.502388

[9] Sebastian Günther, Martin Schmitz, Florian Müller, Jan Riemann, and Max Mühlhäuser. 2017. BYO*: Utilizing 3D Printed Tangible Tools for Interaction on Interactive Surfaces. In *Proceedings of the 2017 ACM Workshop on Interacting with Smart Objects - SmartObject '17*. ACM Press, New York, New York, USA, 21–26. DOI: http://dx.doi.org/10.1145/3038450.3038456

[10] Changyo Han, Katsufumi Matsui, and Takeshi Naemura. 2020. ForceStamps: Fiducial Markers for Pressure-sensitive Touch Surfaces to Support Rapid Porototyping of Physical Control Interfaces. In *Proceedings of the Fourteenth International Conference on Tangible, Embedded, and Embodied Interaction - TEI '20*. DOI:http://dx.doi.org/10.1145/3374920.3374924

[11] Changyo Han and Takeshi Naemura. 2019. BumpMarker: a 3D-printed tangible marker for simultaneous tagging, tracking, and weight measurement. *ITE Transactions on Media Technology and Applications* 7, 1 (2019), 11–19. DOI: http://dx.doi.org/10.3169/mta.7.11

[12] Fabian Hennecke, Franz Berwein, and Andreas Butz. 2011. Optical Pressure Sensing for Tangible User Interfaces. In *Proceedings of the ACM International Conference on Interactive Tabletops and Surfaces - ITS '11*. ACM Press, New York, New York, USA, 45–48. DOI:http://dx.doi.org/10.1145/2076354.2076362

[13] Sanghwa Hong, Eunseok Jeong, Seongkook Heo, and Byungjoo Lee. 2018. FDSense: Estimating Young's Modulus and Stiffness of End Effectors to Facilitate Kinetic Interaction on Touch Surfaces. In *The 31st Annual ACM Symposium on User Interface Software and Technology - UIST '18*. ACM Press, New York, New York, USA, 809–823. DOI: http://dx.doi.org/10.1145/3242587.3242644

[14] Meng-Ju Hsieh, Rong-Hao Liang, Da-Yuan Huang, Jheng-You Ke, and Bing-Yu Chen. 2018. RFIBricks: Interactive Building Blocks Based on RFID. In *Proceedings of the 2018 CHI Conference on Human Factors in Computing Systems - CHI '18*. ACM Press, New York, New York, USA, 1–10. DOI: http://dx.doi.org/10.1145/3173574.3173763

[15] Sungjae Hwang, Myungwook Ahn, and Kwang-yun Wohn. 2013. MagGetz: Customizable Passive Tangible Controllers On and Around Conventional Mobile Devices. In *Proceedings of the 26th annual ACM symposium on User interface software and technology - UIST '13*. ACM Press, New York, New York, USA, 411–416. DOI: http://dx.doi.org/10.1145/2501988.2501991

[16] Kaori Ikematsu and Itiro Siio. 2018. Ohmic-Touch: Extending Touch Interaction by Indirect Touch through Resistive Objects. In *Proceedings of the 2018 CHI Conference on Human Factors in Computing Systems -*

CHI '18. ACM Press, New York, New York, USA, 1–8. DOI:http://dx.doi.org/10.1145/3173574.3174095

[17] Michael D. Jones, Casey Walker, Zann Anderson, Candice Lusk, and Andrew Bryce. 2017. Exploring a Modular Approach to Redesigning Interfaces for Physical Interactive Devices. In *Proceedings of the Tenth International Conference on Tangible, Embedded, and Embodied Interaction - TEI '17*. ACM Press, New York, New York, USA, 465–471. DOI: http://dx.doi.org/10.1145/3024969.3025075

[18] Yasuaki Kakehi, Kensei Jo, Katsunori Sato, Kouta Minamizawa, Hideaki Nii, Naoki Kawakami, Takeshi Naemura, and Susumu Tachi. 2008. ForceTile: Tabletop Tangible Interface with Vision-based Force Distribution Sensing. In *ACM SIGGRAPH 2008 new tech demos on - SIGGRAPH '08*. ACM Press, New York, New York, USA, 1–1. DOI: http://dx.doi.org/10.1145/1401615.1401632

[19] Hyunyoung Kim, Céline Coutrix, and Anne Roudaut. 2018. KnobSlider: Design of a Shape-Changing UI for Parameter Control. In *Proceedings of the 2018 CHI Conference on Human Factors in Computing Systems - CHI '18*. ACM Press, New York, New York, USA, 1–13. DOI:http://dx.doi.org/10.1145/3173574.3173913

[20] Gierad Laput, Eric Brockmeyer, Scott E. Hudson, and Chris Harrison. 2015. Acoustruments: Passive, Acoustically-Driven, Interactive Controls for Handheld Devices. In *Proceedings of the 33rd Annual ACM Conference on Human Factors in Computing Systems - CHI '15*. ACM Press, New York, New York, USA, 2161–2170. DOI: http://dx.doi.org/10.1145/2702123.2702414

[21] Johnny C. Lee, Daniel Avrahami, Scott E. Hudson, Jodi Forlizzi, Paul H. Dietz, and Darren Leigh. 2004. The Calder Toolkit: Wired and Wireless Components for Rapidly Prototyping Interactive Devices. In *Proceedings of the 2004 conference on Designing interactive systems processes, practices, methods, and techniques - DIS '04*. ACM Press, New York, New York, USA, 167. DOI: http://dx.doi.org/10.1145/1013115.1013139

[22] Jakob Leitner and Michael Haller. 2011. Geckos: Combining Magnets and Pressure Images to Enable New Tangible-object Design and Interaction. In *Proceedings of the 2011 annual conference on Human factors in computing systems - CHI '11*. ACM Press, New York, New York, USA, 2985–2994. DOI: http://dx.doi.org/10.1145/1978942.1979385

[23] Rong-Hao Liang, Liwei Chan, Hung-Yu Tseng, Han-Chih Kuo, Da-Yuan Huang, De-Nian Yang, Bing-Yu Chen, Rong-Hao Liang, Liwei Chan, Hung-Yu Tseng, Han-Chih Kuo, Da-Yuan Huang, De-Nian Yang, and Bing-Yu Chen. 2014a. GaussBricks: Magnetic Building Blocks for Constructive Tangible Interactions on Portable Displays. In *Proceedings of the 32nd annual ACM conference on Human factors in computing systems - CHI '14*. ACM Press, New York, New York, USA, 3153–3162. DOI: http://dx.doi.org/10.1145/2556288.2557105

[24] Rong-Hao Liang, Han-Chih Kuo, Liwei Chan, De-Nian Yang, and Bing-Yu Chen. 2014b. GaussStones: Shielded Magnetic Tangibles for Multi-Token Interactions on Portable Displays Rong-Hao. In *Proceedings of the 27th annual ACM symposium on User interface software and technology - UIST '14*. ACM Press, New York, New York, USA, 365–372. DOI: http://dx.doi.org/10.1145/2642918.2647384

[25] Satoshi Nakamaru, Ryosuke Nakayama, Ryuma Niiyama, and Yasuaki Kakehi. 2017. FoamSense: Design of Three Dimensional Soft Sensors with Porous Materials. In *UIST 2017 - Proceedings of the 30th Annual ACM Symposium on User Interface Software and Technology*. ACM Press, New York, New York, USA, 437–447. DOI: http://dx.doi.org/10.1145/3126594.3126666

[26] Ryosuke Nakayama, Ryo Suzuki, Satoshi Nakamaru, Ryuma Niiyama, Yoshihiro Kawahara, and Yasuaki Kakehi. 2019. MorphIO: Entirely Soft Sensing and Actuation Modules for Programming Shape Changes through Tangible Interaction. In *Proceedings of the 2019 on Designing Interactive Systems Conference - DIS '19*. ACM Press, New York, New York, USA, 975–986. DOI: http://dx.doi.org/10.1145/3322276.3322337

[27] Simon Olberding, Sergio Soto Ortega, Klaus Hildebrandt, and Jürgen Steimle. 2015. Foldio: Digital Fabrication of Interactive and Shape- Changing Objects With Foldable Printed Electronics. In *Proceedings of the 28th Annual ACM Symposium on User Interface Software & Technology - UIST '15*. ACM Press, New York, New York, USA, 223–232. DOI: http://dx.doi.org/10.1145/2807442.2807494

[28] James Patten, Hiroshi Ishii, Jim Hines, and Gian Pangaro. 2001. Sensetable: a wireless object tracking platform for tangible user interfaces. In *Proceedings of the SIGCHI conference on Human factors in computing systems - CHI '01*. ACM Press, New York, New York, USA, 253–260. DOI: http://dx.doi.org/10.1145/365024.365112

[29] Parinya Punpongsanon, Daisuke Iwai, and Kosuke Sato. 2014. Projection-based visualization of tangential deformation of nonrigid surface by deformation estimation using infrared texture. *Virtual Reality* 19, 1 (2014), 45–56. DOI: http://dx.doi.org/10.1007/s10055-014-0256-y

[30] Simon Robinson, Céline Coutrix, Jennifer Pearson, Juan Rosso, Matheus Fernandes Torquato, Laurence Nigay, and Matt Jones. 2016. Emergeables: Deformable Displays for Continuous Eyes-Free Mobile Interaction. In *Proceedings of the 2016 CHI Conference on Human Factors in Computing Systems - CHI '16*. ACM Press, New York, New York, USA, 3793–3805. DOI: http://dx.doi.org/10.1145/2858036.2858097

[31] Valkyrie Savage, Ryan Schmidt, Tovi Grossman, George Fitzmaurice, and Björn Hartmann. 2014. A Series of Tubes: Adding Interactivity to 3D Prints Using Internal Pipes. In *Proceedings of the 27th annual ACM symposium on User interface software and technology - UIST '14*. ACM Press, New York, New York, USA, 3–12. DOI:http://dx.doi.org/10.1145/2642918.2647374

[32] Dominik Schmidt, Christoph Sterz, Yanina Yurchenko, Patrick Baudisch, Raf Ramakers, Esben W. Pedersen, Johannes Jasper, Sven Köhler, Aileen Pohl, Hannes Rantzsch, Andreas Rau, and Patrick Schmidt. 2014. Kickables: Tangibles for Feet. In *Proceedings of the 32nd annual ACM conference on Human factors in computing systems - CHI '14*. ACM Press, New York, New York, USA, 3143–3152. DOI: http://dx.doi.org/10.1145/2556288.2557016

[33] Martin Schmitz, Jürgen Steimle, Jochen Huber, Niloofar Dezfuli, and Max Mühlhäuser. 2017. Flexibles: Deformation-Aware 3D-Printed Tangibles for Capacitive Touchscreens. In *Proceedings of the 2017 CHI Conference on Human Factors in Computing Systems - CHI '17*. ACM Press, New York, New York, USA, 1001–1014. DOI: http://dx.doi.org/10.1145/3025453.3025663

[34] Timothy M. Simon, Bruce H. Thomas, Ross T. Smith, and Mark Smith. 2013. Adding Input Controls and Sensors to RFID Tags to support Dynamic Tangible User Interfaces. In *Proceedings of the 8th International Conference on Tangible, Embedded and Embodied Interaction - TEI '14*. ACM Press, New York, New York, USA, 165–172. DOI: http://dx.doi.org/10.1145/2540930.2540979

[35] Ronit Slyper and Jessica Hodgins. 2012. Prototyping Robot Appearance, Movement, and Interactions Using Flexible 3D Printing and Air Pressure Sensors. In *2012 IEEE RO-MAN: The 21st IEEE International Symposium on Robot and Human Interactive Communication*. IEEE, 6–11. DOI: http://dx.doi.org/10.1109/ROMAN.2012.6343723

[36] Paul Strohmeier, Victor Håkansson, Cedric Honnet, Daniel Ashbrook, and Kasper Hornbæk. 2019. Optimizing Pressure Matrices: Interdigitation and Interpolation Methods for Continuous Position Input. In *Proceedings of the Thirteenth International Conference on Tangible, Embedded, and Embodied Interaction - TEI '19*. ACM Press, New York, New York, USA, 117–126. DOI:http://dx.doi.org/10.1145/3294109.3295638

[37] Yuta Sugiura, Calista Lee, Masayasu Ogata, Anusha Withana, Yasutoshi Makino, Daisuke Sakamoto, Masahiko Inami, and Takeo Igarashi. 2012. PINOKY: A Ring That Animates Your Plush Toys. In *Proceedings of the 2012 ACM annual conference on Human Factors in Computing Systems - CHI '12*. ACM Press, New York, New York, USA, 725. DOI: http://dx.doi.org/10.1145/2207676.2207780

[38] Koray Tahiroğlu, Thomas Svedström, Valtteri Wikström, Simon Overstall, Johan Kildal, and Teemu Ahmaniemi. 2014. SoundFLEX: Designing Audio to Guide Interactions with Shape-Retaining Deformable Interfaces. In *Proceedings of the 16th International Conference on Multimodal Interaction - ICMI '14*. ACM Press, New York, New York, USA, 267–274. DOI: http://dx.doi.org/10.1145/2663204.2663278

[39] Giovanni Maria Troiano, Esben Warming Pedersen, and Kasper Hornbæk. 2015. Deformable Interfaces for Performing Music. In *Proceedings of the 33rd Annual ACM Conference on Human Factors in Computing Systems - CHI '15*. ACM Press, New York, New York, USA, 377–386. DOI: http://dx.doi.org/10.1145/2702123.2702492

[40] Bert Vandenberghe, Kathrin Gerling, Luc Geurts, and Vero Vanden Abeele. 2019. Skweezee for Processing: A Software Library to Make Squeeze Interactions. In *Proceedings of the Thirteenth International Conference on Tangible, Embedded, and Embodied Interaction - TEI '19*. ACM Press, New York, New York, USA, 375–381. DOI:http://dx.doi.org/10.1145/3294109.3300984

[41] Marynel Vázquez, Eric Brockmeyer, Ruta Desai, Chris Harrison, and Scott E. Hudson. 2015. 3D Printing Pneumatic Device Controls with Variable Activation Force Capabilities. In *Proceedings of the 33rd Annual ACM Conference on Human Factors in Computing Systems - CHI '15*. ACM Press, New York, New York, USA, 1295–1304. DOI: http://dx.doi.org/10.1145/2702123.2702569

[42] Nicolas Villar and Hans Gellersen. 2007. A Malleable Control Structure for Softwired User Interfaces. In *Proceedings of the 1st international conference on Tangible and embedded interaction - TEI '07*. ACM Press, New York, New York, USA, 49–56. DOI: http://dx.doi.org/10.1145/1226969.1226980

[43] Nicolas Villar, Haiyan Zhang, Daniel Cletheroe, Greg Saul, Christian Holz, Tim Regan, Oscar Salandin, Misha Sra, Hui-Shyong Yeo, and William Field. 2018. Project Zanzibar: A Portable and Flexible Tangible Interaction Platform. In *Proceedings of the 2018 CHI Conference on Human Factors in Computing Systems - CHI '18*. ACM Press, New York, New York, USA, 1–13. DOI: http://dx.doi.org/10.1145/3173574.3174089

[44] Simon Voelker, Christian Cherek, Jan Thar, Thorsten Karrer, Christian Thoresen, Kjell Ivar Øvergård, and Jan Borchers. 2015. PERCs: Persistently Trackable Tangibles on Capacitive Multi-Touch Displays. In *Proceedings of the 28th Annual ACM Symposium on User Interface Software & Technology - UIST '15*. ACM Press, New York, New York, USA, 351–356. DOI: http://dx.doi.org/10.1145/2807442.2807466

[45] Malte Weiss, Julie Wagner, Yvonne Jansen, Roger Jennings, Ramsin Khoshabeh, James D. Hollan, and Jan Borchers. 2009. SLAP widgets: bridging the gap between virtual and physical controls on tabletops. In *Proceedings of the 27th international conference on*

Human factors in computing systems - CHI 09. ACM Press, New York, New York, USA, 481. DOI: http://dx.doi.org/10.1145/1518701.1518779

[46] Lining Yao, Ryuma Niiyama, Jifei Ou, Sean Follmer, Clark Della Silva, and Hiroshi Ishii. 2013. PneUI: pneumatically actuated soft composite materials for shape changing interfaces. In *ACM Transactions on Graphics*. ACM Press, New York, New York, USA, 13–22. DOI:http://dx.doi.org/10.1145/2501988.2502037

[47] Sang Ho Yoon, Luis Paredes, Ke Huo, and Karthik Ramani. 2018. MultiSoft: Soft Sensor Enabling Real-Time Multimodal Sensing with Contact Localization and Deformation Classification. *Proc. ACM Interact. Mob. Wearable Ubiquitous Technol.* 2, 3 (2018), 1–22. DOI:http://dx.doi.org/10.1145/3264955

[48] Neng-Hao Yu, Polly Huang, Yi-Ping Hung, Li-Wei Chan, Seng Yong Lau, Sung-Sheng Tsai, I-Chun Hsiao, Dian-Je Tsai, Fang-I Hsiao, Lung-Pan Cheng, and Mike Chen. 2011. TUIC: Enabling Tangible Interaction on Capacitive Multi-touch Display. In *Proceedings of the 2011 annual conference on Human factors in computing systems - CHI '11*. ACM Press, New York, New York, USA, 2995–3004. DOI: http://dx.doi.org/10.1145/1978942.1979386

[49] Yuan-Fang Zhang, Colin Ju-Xiang Ng, Zhe Chen, Wang Zhang, Sahil Panjwani, Kavin Kowsari, Hui Ying Yang, and Qi Ge. 2019. Miniature Pneumatic Actuators for Soft Robots by High-Resolution Multimaterial 3D Printing. *Advanced Materials Technologies* 1900427 (8 2019), 1–9. DOI: http://dx.doi.org/10.1002/admt.201900427